

Article

Luminescent and Scintillation Properties of CeAlO₃ Crystals and Phase-Separated CeAlO₃/CeAl₁₁O₁₈ Metamaterials

Oleg Sidletskiy ^{1,*}, Pavlo Arhipov ¹, Serhii Tkachenko ¹, Iaroslav Gerasymov ¹ ,
Georgiy Trushkovsky ¹, Tetyana Zorenko ², Yuriy Zorenko ² , Pavel Mateychenko ³,
Anna Puzan ⁴ , Wojciech Gieszczyk ⁵ and Pawel Bilski ⁵ 

¹ Institute for Scintillation Materials, National Academy of Sciences of Ukraine, 61072 Kharkiv, Ukraine; arhipovisma@gmail.com (P.A.); tkachenko2835@gmail.com (S.T.); yarosgerasimov@gmail.com (I.G.); geotrush@gmail.com (G.T.)

² Institute of Physics, Kazimierz Wielki University in Bydgoszcz, 85090 Bydgoszcz, Poland; tzorenko@ukw.edu.pl (T.Z.); zorenko@ukw.edu.pl (Y.Z.)

³ Institute for Single Crystals, National Academy of Sciences of Ukraine, Kharkiv 61072, Ukraine; paul@isc.kharkov.ua

⁴ SSI Institute for Single Crystals, National Academy of Sciences of Ukraine, 61072 Kharkiv, Ukraine; annapuzan199114@gmail.com

⁵ Institute of Nuclear Physics, Polish Academy of Sciences, 31342 Krakow, Poland; wojciech.gieszczyk@gmail.com (W.G.); pawel.bilski@ifj.edu.pl (P.B.)

* Correspondence: osidletskiy@yahoo.com; Tel.: +380-57-341-0366

Received: 29 April 2019; Accepted: 4 June 2019; Published: 6 June 2019



Abstract: This work is dedicated to the growth process and investigation of luminescent and scintillation properties of CeAlO₃ single crystals and CeAlO₃/CeAl₁₁O₁₈ metamaterials under e-beam and α -particles excitation. It has been shown that cathodoluminescence and radioluminescence spectra of CeAlO₃ crystals contain two bands, peaking at 440 and 500 nm, and caused by the Ce³⁺ 5d–4f transitions into CeAl₁₁O₁₈ phase, which is present in these crystals as an admixture. Under 270 nm ultraviolet (UV) light excitation, a CeAlO₃ crystal possesses complicated non-exponential luminescence decay, with the average decay time of 16 ns. The light yield of CeAlO₃ crystals under α -particle excitation is about 16% and 12%, in respect to the standard Bi₄Ge₃O₁₂ (BGO) crystal and Y₃Al₅O₁₂:Ce (YAG:Ce) single crystalline film samples, respectively. The CeAlO₃ scintillation decay is quite fast, with the decay time value $t_{1/e}$ in the 54–56 ns range.

Keywords: CeAlO₃ crystals; CeAlO₃/CeAl₁₁O₁₈ metamaterials; luminescence; scintillators

1. Introduction

An interest in CeAlO₃ crystals has been prompted by their ferroelectric, optical, and luminescent properties and the possibility to apply them as solid electrolytes, gaseous gauges, and catalysts [1]. Because of the complex obtaining procedure, before 2015, CeAlO₃ crystals could only be made in powder or microcrystalline form. Recently, the procedure of obtaining bulk crystals by the Czochralski and edge-defined film-fed grown (EFG) methods has been developed [2]. These have opened wider perspectives for CeAlO₃ application. As this material contains trivalent cerium, one of the most efficient activators of fast luminescence in scintillators, information on CeAlO₃ luminescence and scintillation properties should be updated and reconsidered. The luminescence response of both CeAlO₃ ceramics and some colored bulk crystals has been recorded under UV-irradiation. However, no emission under X-ray and gamma-excitation was observed [2]. Meanwhile, the luminescence properties of

CeAlO₃ crystals under excitation with higher ionization density, such as cathodoluminescence, α - and β -particles, have not been studied yet.

The Ce₂O₃-Al₂O₃ system also enables the preparation of metaphase columnar compositions. Such structures are known as eutectic metamaterials or phase-separated crystals [3]. As the examples, the binary GdAlO₃:Ce/Al₂O₃ [4], CsI/NaCl and related systems [5], and LiF/CaF₂/LiBaF₃ ternary system [6] were introduced. Such metamaterials can be crystallized from eutectic compositions, and their grain size and quantity can be controlled by the growth rate and the melt composition [5]. The phase separation therein includes columns of a first, emitting crystal phase incorporated into the host of a second crystal phase having a higher refractive index than that of the first crystal phase to provide a light guide function. A unidirectional phase-separated structure provides a light guide function for crosstalk prevention without using partitions. It can be useful, for example, in computer tomography (CT) scanners with high spatial resolution.

This work overviews an obtaining procedure of the ordered CeAlO₃/CeAl₁₁O₁₈ metaphase structures, as well as the study of the luminescence properties of CeAlO₃ crystals and CeAlO₃/CeAl₁₁O₁₈ structures under excitation by selective UV light, e-beam, α - and β -particles, and high-energy X-ray quanta.

2. Materials and Methods

2.1. Fabrication of CeAlO₃ Samples

CeAlO₃ bulk crystals were grown on a CeAlO₃ seed by the EFG method from tungsten (W) crucibles in an Ar + CO reducing atmosphere. A raw material with the stoichiometric CeAlO₃ composition was synthesized from 99.99% purity (4N-grade) CeO₂ and Al₂O₃ powders under the same reducing atmosphere. Crystals were pulled from the melt at a rate of 3–7 mm/hour. The length of ingots was up to 100 mm and the cross section was up to 2 × 20 mm². The crystal growth procedure was described in detail in [2]. The melting point of CeAlO₃ is around 2050 °C [2]. The samples were extracted from the grown ingots and polished for optical and scintillation measurements. Then some samples were annealed at 1300 °C under an Ar and CO reducing atmosphere, or in a vacuum.

2.2. Phase Analysis

Structure and phase composition were determined with a Siemens D500 diffractometer. In prior study [2] X-ray diffraction (XRD) analysis of single crystalline samples did not show any admixture phases, except the CeAlO₃ tetragonal phase, space group I4/mcm, though reflections similar to the isostructural LaAl₁₁O₁₈ phase were obtained in the sintered raw material.

2.3. Element Analysis

The surface composition of the studied samples, with the relative error $\pm 1\%$, was controlled using a JSM 6390 LVX (Peabody, MA, USA) scanning electron microscope (SEM) with the MAX^N X-ray microanalysis system. Structure and phase composition of samples were determined using a Siemens D500 diffractometer (Berlin, Germany). The phases were identified using EVA and SEARCH software and the PDF-1 database.

2.4. Luminescent and Scintillation Measurements

All luminescent and scintillation measurements were carried out at room temperature (RT). The cathodoluminescence (CL) spectra were measured using a SEM JEOL JSM-820 electron microscope (Peabody, MA, USA) equipped with a Stellar Net spectrometer and TE-cooled CCD detector working in the 200–925 nm range. The scintillation light yield (LY), and luminescence decay measurements were performed with a shaping time of 12 μ s using the setup based on a Hamamatsu H6521 PMP, multi-channel analyzer and digital TDS3052 oscilloscope under excitation by α -particles of a Pu²³⁹ (5.15 MeV) source. The photoluminescence (PL) emission and excitation spectra of the crystals

were measured using an Edinburgh Instruments FS5 spectrofluorometer. For thermal stimulated luminescence (TSL) of the samples under study, we used an automatic Risø TL/OSL-DA20 reader (Roskilde, Denmark) and excitations by α -particles (500 s; 49.976 Gy, ^{241}Am source) and β -particles (10 s; 0.97 Gy, $^{90}\text{Sr}/^{90}\text{Y}$ source).

3. Results and Discussion

3.1. Structure and Composition of CeAlO_3 Crystals and $\text{CeAlO}_3/\text{CeAl}_{11}\text{O}_{18}$ Metaphase Systems

As-grown CeAlO_3 single crystals are colored as shown in Figure 1a. The coloration disappears after 2–4 h of post-growth annealing at 1300 °C in the Ar and CO reducing atmosphere. Meanwhile, we noticed that the bleaching process is not uniform in the crystal bulk, and some colored spots remain at the surface at intermediate stage (Figure 1b). The photos of the studied colored and transparent samples are presented in Figure 1.

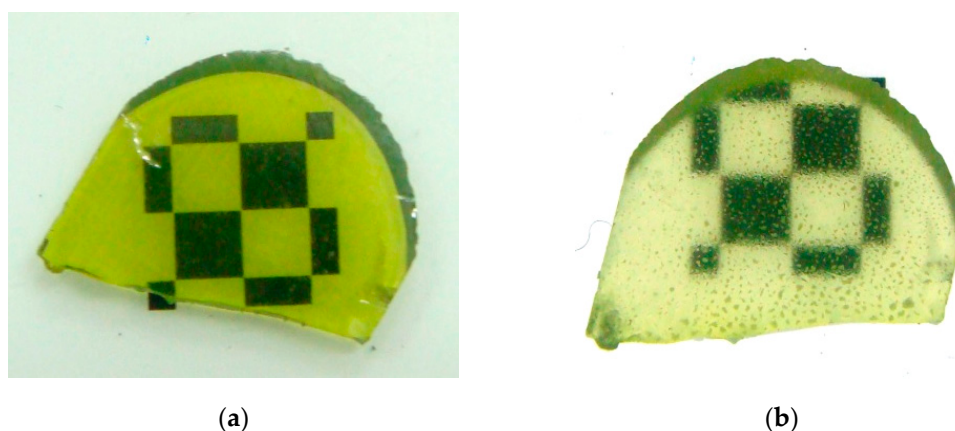


Figure 1. CeAlO_3 single crystalline samples before (a) and after (b) annealing at 1700 °C in the Ar and CO reducing atmosphere.

Some ingots were polycrystalline (Figure 2a,b) and show a visible emission under UV light irradiation, as seen in Figure 2c. Microanalysis showed that while the light-emitting areas have composition around $\text{Ce}_{0,2}\text{Al}_{1,8}\text{O}_3$, the composition of other grains was between $\text{Ce}_{1,1}\text{Al}_{0,9}\text{O}_3$ and $\text{Ce}_{1,2}\text{Al}_{0,8}\text{O}_3$. This almost corresponds to $\text{CeAl}_{11}\text{O}_{18}$ in the light-emitting grains and CeAlO_3 in the rest of the grains.

The XRD data (Figure 3) show the presence of a small amount of $\text{CeAl}_{11}\text{O}_{18}$ phase in addition to the main CeAlO_3 phase. No evidence of other phases have been obtained. From SEM images (Figure 4a), it can clearly be seen that the cut of EGF-grown crystal contains $\text{CeAl}_{11}\text{O}_{18}$ phase inclusions (light areas) arranged into columns oriented along the different directions and embedded into the CeAlO_3 host phase (dark areas). Under higher resolution (Figure 4b), one can see the $\text{CeAl}_{11}\text{O}_{18}$ columns of oval shape with the 3–5 μm size are surrounded by smaller grains with the size less than 1 μm and composition around CeAlO_3 .

As the eutectic composition between CeAlO_3 and $\text{CeAl}_{11}\text{O}_{18}$ is $\text{Ce}_{0,46}\text{Al}_{1,54}\text{O}_3$ [7], the Al_2O_3 content has to be increased for directional synthesis of the phase-separated columnar structure. While in the shown crystals, phase-separated structures were occasionally formed, such structures can be formed intentionally by a shift of melt composition, or by solid phase synthesis. The latter was implemented in this work by the annealing of visually homogeneous CeAlO_3 crystals in contact with a single Al_2O_3 crystal at 1700 °C. While the composition of the crystal surface before the annealing was precisely CeAlO_3 , after annealing, the surface integral composition shifted to $\text{Ce}_{0,38}\text{Al}_{1,62}\text{O}_3$. Herein, the measured compositions of the light and dark areas in Figure 5 are $\text{Ce}_{0,54}\text{Al}_{1,46}\text{O}_3$, and $\text{Ce}_{0,26}\text{Al}_{1,74}\text{O}_3$, correspondingly, with larger and smaller Ce/Al ratios relative to the $\text{Ce}_{0,46}\text{Al}_{1,54}\text{O}_3$ eutectic composition. The compositions of light and dark areas are close to CeAlO_3 and $\text{CeAl}_{11}\text{O}_{18}$,

because the spatial resolution of the method is limited by $1\ \mu\text{m}$ and it is barely possible to determine the composition of a single $\sim 1\ \mu\text{m}$ size area. This picture is very similar to the microstructure of the $\text{Tb}_3\text{Sc}_2\text{Al}_3\text{O}_{12}\text{-TbScO}_3$ binary eutectic grown by the micro-pulling down method [3]. As no data on CeAlO_3 and $\text{CeAl}_{11}\text{O}_{18}$ refractive indices are known at the moment, it is not possible to evaluate precisely the wave guiding properties of such columnar structure. However, the bright emission from the $\text{CeAl}_{11}\text{O}_{18}$ -designated areas and the high refraction index of 1.98 in LaAlO_3 homologue with perovskite structure [8] provides evidence that the $\text{CeAl}_{11}\text{O}_{18}$ refractive index is lower.

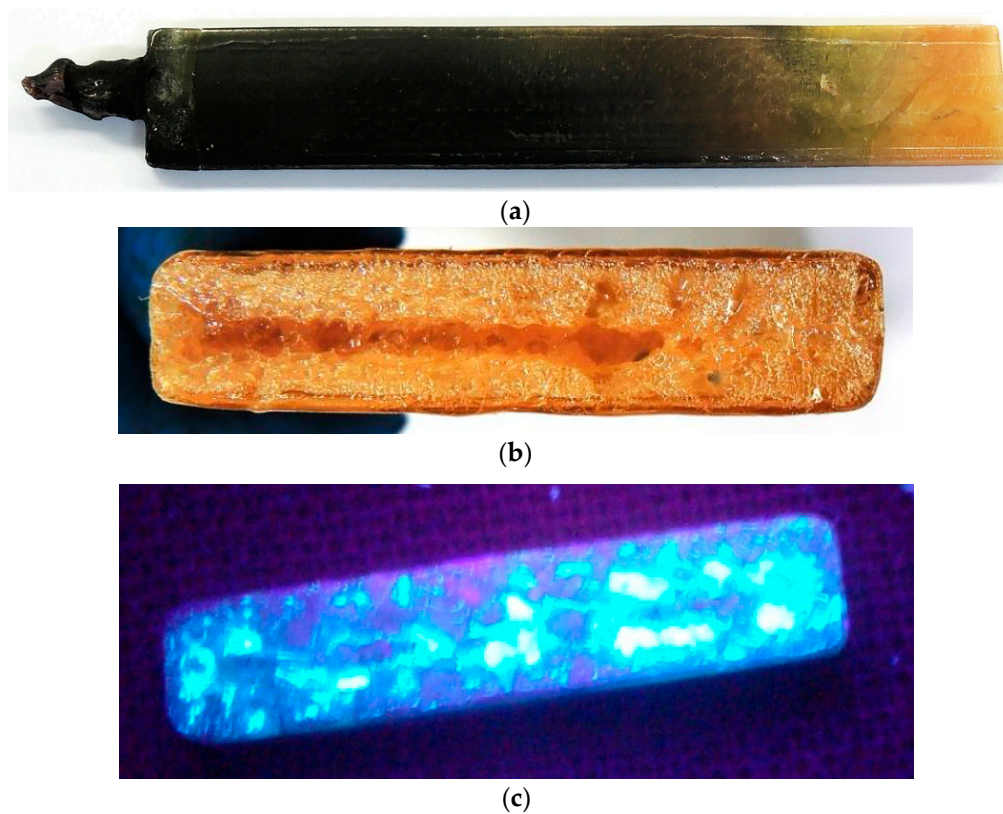


Figure 2. Photos of as-grown crystal (a), its transversal cut (b), and the same transversal cut under illumination with UV light (c).

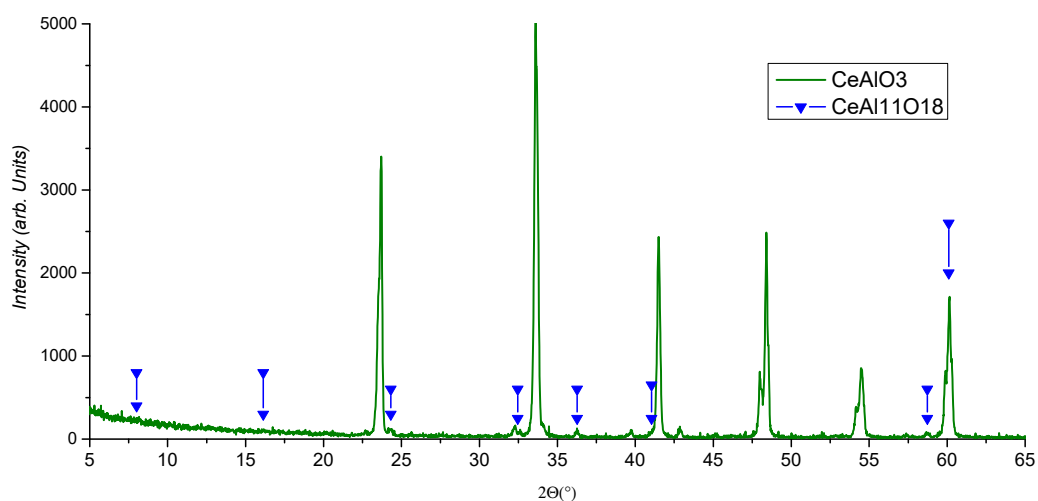


Figure 3. XRD of the transverse cut of polycrystalline sample grown by the edge-defined film-fed (EFG) technique.

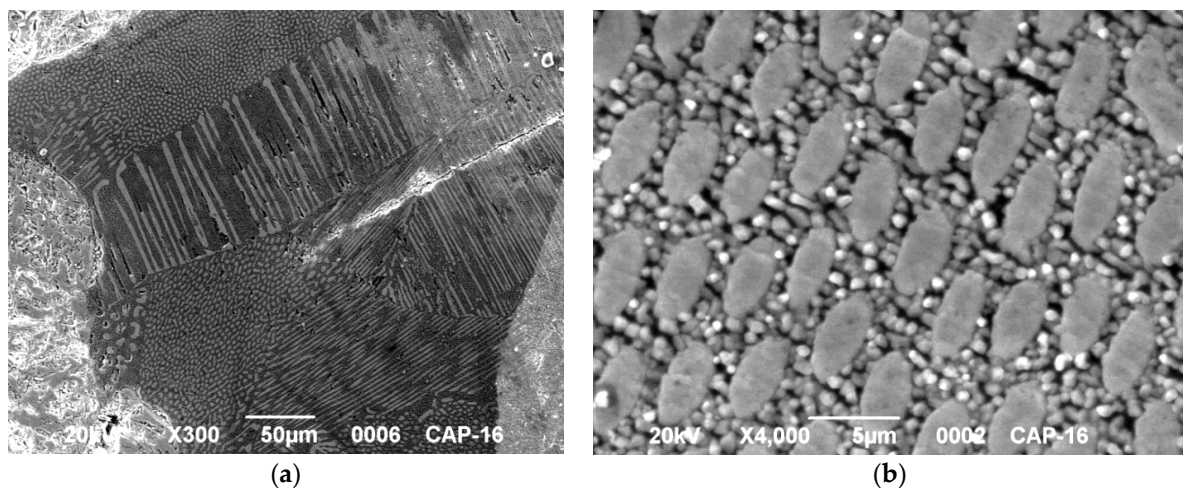


Figure 4. SEM images of crystallites at the transverse cut: (a) $\times 300$ magnification; (b) $\times 4000$ magnification.

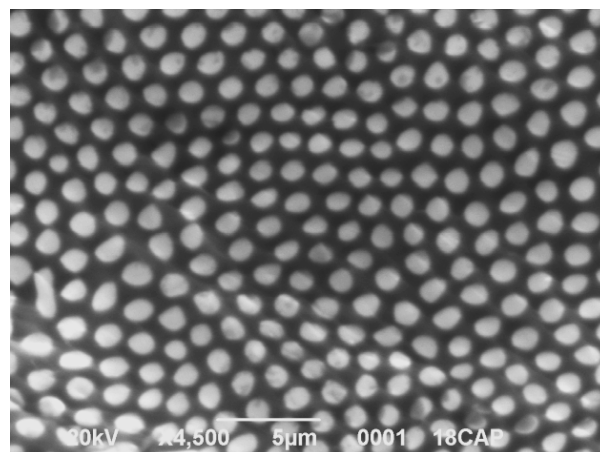


Figure 5. SEM image (magnification $\times 4500$) of the eutectic structure at the surface of CeAlO_3 crystal annealed at 1700°C under vacuum in contact with Al_2O_3 crystal.

3.2. Optical and Luminescent Properties

The absorption spectra of as-grown and annealed samples are presented in Figure 6. Absorption of the as-grown CeAlO_3 crystals is characterized by the main band peaking at 420 nm. As this band completely disappears after annealing in an Ar + CO reducing atmosphere (Figure 6, curve 2), eventually promoting the $\text{Ce}^{4+} \rightarrow \text{Ce}^{3+}$ transfer, it is likely that this band is related to $\text{O}^{2-} \rightarrow \text{Ce}^{4+}$ charge transfer transitions in the CeAlO_3 host, similar to other Ce-containing materials [9].

The luminescence of CeAlO_3 crystals under excitation by e-beam and α - and β -particles was registered for the first time (Figure 7). Under e-beam excitation, the observed double luminescence band in CeAlO_3 crystals, peaking at 446 and 500 nm, is probably related to the Ce^{3+} 5d-4f transition into the $\text{CeAl}_{11}\text{O}_{18}$ admixture phase. The CL intensity is significantly larger in the annealed sample due to the increase of Ce^{3+} -emitting centers concentration and the decrease of luminescence reabsorption by the CT-related absorption band, which peaked at 420 nm (see Figure 7).

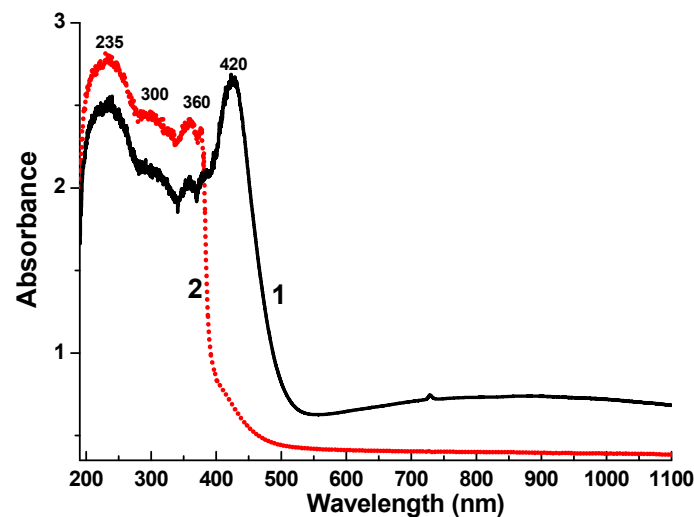


Figure 6. Absorption spectra of as-grown (1) and annealed (2) CeAlO_3 single crystals with a thickness of 1 mm.

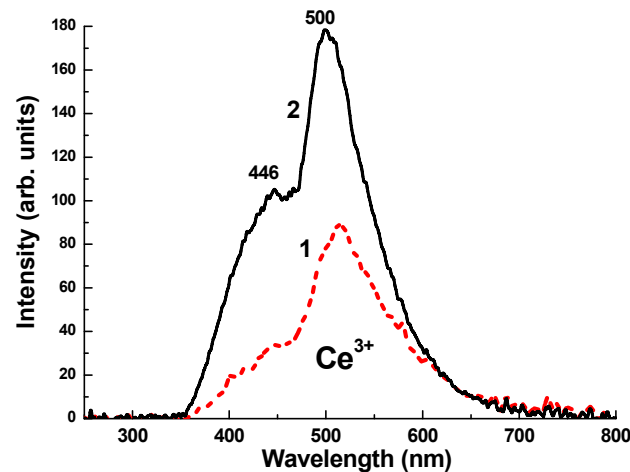


Figure 7. Cathodoluminescence spectra of CeAlO_3 single crystals: 1, as-grown; 2, annealed.

However, we noticed that in annealed CeAlO_3 crystals, the UV-excited blue photoluminescence is emitted not from the overall volume of the CeAlO_3 bulk crystal, but mainly from colored spots (see Figure 1b). The shapes of the photoluminescence spectra of the spots at the crystal surface and sintered raw material powders are similar (Figure 8), which points to the emission of $\text{CeAl}_{11}\text{O}_{18}$ phase embedded in the CeAlO_3 crystals, as suggested in [2].

Indeed, the comparison of UV-excited photoluminescence spectra of the metaphase structure and colored spots at the transparent CeAlO_3 crystal surface (Figure 8) confirms the similar nature of the luminescence response. At 260–265 nm excitation, a wide band with the main peaks near 430–450 and 504–508 nm is observed. Therefore, we attribute the UV-excited luminescence in CeAlO_3 crystal to the $\text{CeAl}_{11}\text{O}_{18}$ phase admixture in the raw material powders, as well as in the single- and polycrystalline samples.

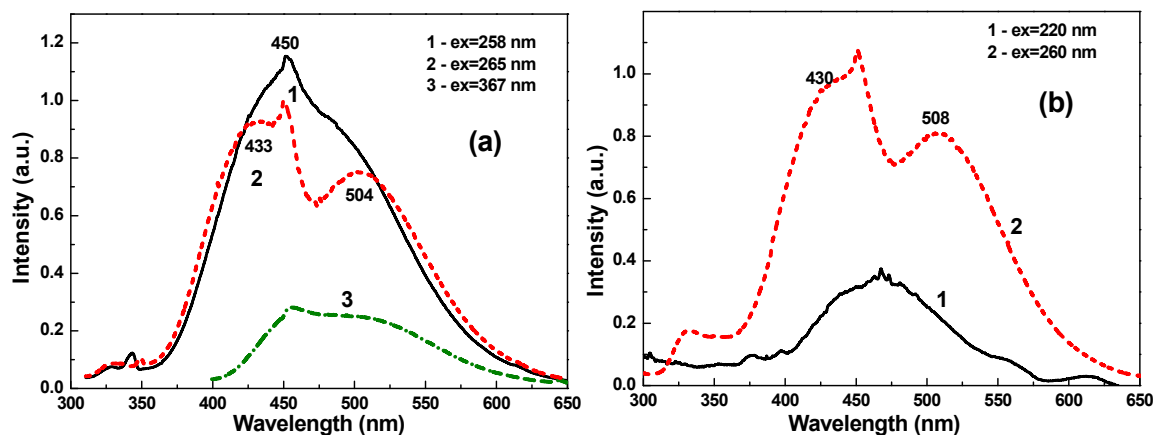


Figure 8. Luminescence spectra of CeAlO_3 eutectic structure (a) and colored spots at the surface of transparent CeAlO_3 single crystal and (b) under excitation with the different wavelengths in the UV range.

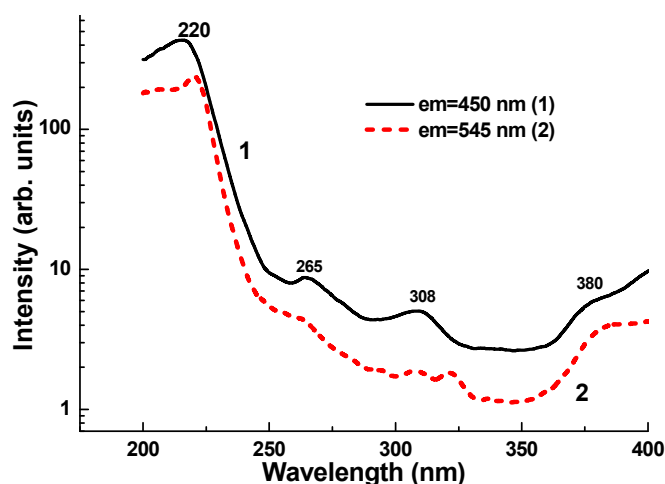


Figure 9. Photoluminescence excitation spectra of a CeAlO_3 crystal. Annealed sample monitored at 450 nm (1) and annealed CeAlO_3 crystal monitored at 545 nm (2).

Excitation spectra of these main luminescence bands are of quite similar shape (Figure 9). Several distinguished peaks at 220, 265, and 308 nm, as well as the complex peaks at 380 nm, show that the excitation spectra are related to 4f–5d transitions in Ce^{3+} ions. Most probably, these two group of excitation bands are connected to the transition from the $^2F_{5/2}$ level of ground state to the 2E and T_{2g} excited levels of Ce^{3+} ions in the $\text{CeAl}_{11}\text{O}_{18}$ host. However, such conclusions need more careful experimental confirmation.

The luminescence decay curves of annealed CeAlO_3 crystal sample are shown in Figure 10. Generally, the decay curves monitored at 480 and 540 nm under UV excitation and at 270 nm are quite similar to each other and strongly not exponential. Such shape of the decay curves points at Ce^{3+} luminescence quenching due to some non-radiative process. For this reason we have calculated the average time $t_{1/e}$ of the photoluminescence intensity decay to 1/e level. This value is equal to 16 ns (Figure 10) and is typical for the Ce^{3+} decay time in perovskite hosts [10].

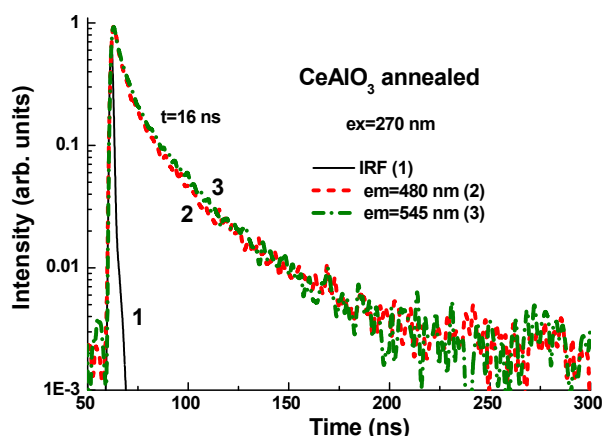


Figure 10. Normalized PL decay of annealed CeAlO_3 crystals under excitation at 270 nm and registration of emission at 480 nm (2) and 540 nm (3). (1) Instrumental response function (IRF) of laser pulse.

3.3. Scintillation Properties of CeAlO_3 Single Crystals

Apart from the fact that the CeAlO_3 single and polycrystals possess very weak luminescence at room temperature under soft X-rays and γ -radiation [2], the scintillation light yield and scintillation decay of CeAlO_3 crystals under α -particle excitation can be seen. Namely, under α -particle excitation by ^{239}Pu sources (5.15 MeV), the light yield of annealed CeAlO_3 crystals is equal to about 16% and 12% in respect to the standard BGO crystal and YAG:Ce SCF sample with the light yields of 1950 and 2600 photon/MeV, respectively. The scintillation response of the annealed CeAlO_3 crystal is quite fast, and the respective scintillation decay time is equal to 56 ns (Figure 11).

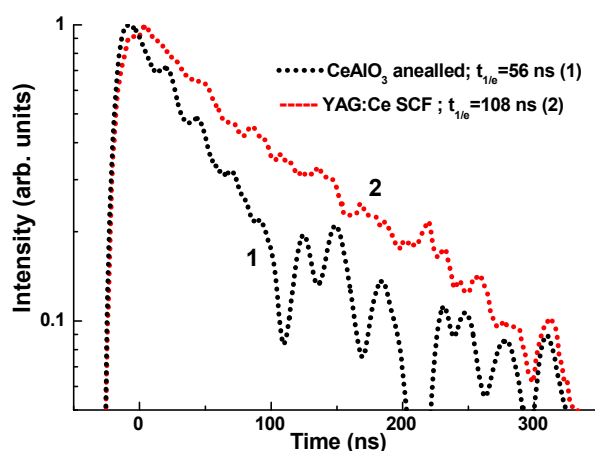


Figure 11. Normalized scintillation decay curves of annealed CeAlO_3 crystals under α -particle excitation of ^{239}Pu sources in comparison with a YAG:Ce SCF standard sample (2).

3.4. Thermoluminescence

CeAlO_3 single crystals after irradiation by high-energy X-rays and α -particles show weak thermoluminescence (TL, Figure 12a). Indeed, the TL peaks in the 120–150 °C and 220–225 °C ranges were resolved mainly after β -particle irradiation (Figure 12a). Meanwhile, after annealing in the reduced atmosphere, the 150 °C peak intensity increased by 6 times after irradiation with β -particles, while the 220 °C peak intensity remained the same (Figure 12b). It is worth noting that after α -particle irradiation, the 150 and 225 K peaks' intensities also increased non-proportionally by 6.26 and 3.8 times, respectively.

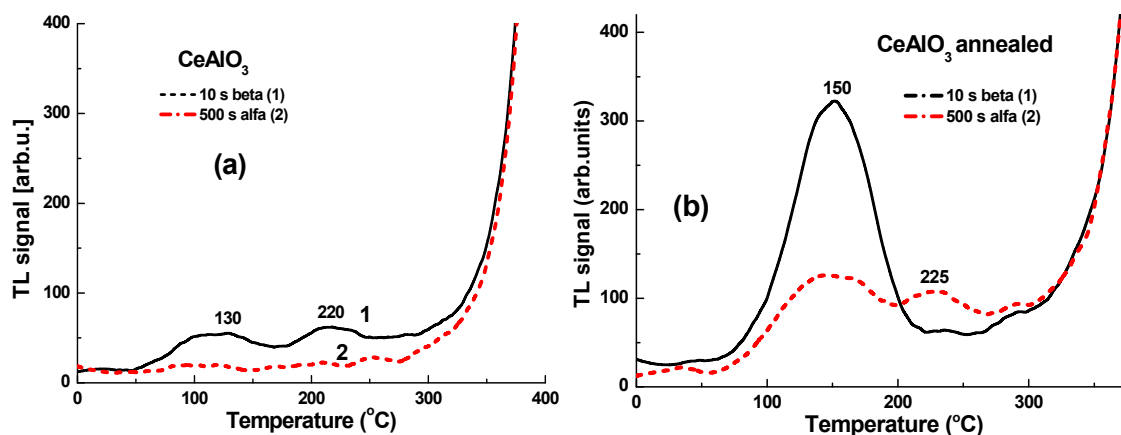


Figure 12. Thermoluminescence (TL) glow curves of as-grown (a) and annealed (b) CeAlO_3 crystals after α - and β - particle excitation with ^{239}Pu (1) and $^{90}\text{Sr}/^{90}\text{Y}$ (2) sources.

Taking into account that Ce^{3+} ions typically serve as the hole trapping centers, the observed TL peaks in the 130–150 °C and 220–225 °C ranges correspond to electron trapping centers. The defects responsible for such deep centers in CeAlO_3 single crystals could be oxygen vacancies trapping one or two electrons (F^+ and F centers, respectively). We can suppose that the concentration of oxygen vacancies is low in as-grown CeAlO_3 crystals, and this fact caused the very weak TL signal in this sample (Figure 12a). Meanwhile, after annealing under the reduction atmosphere, the concentration of oxygen vacancies and related F^+ and F centers could significantly increase. That may lead to the observed TL intensity increase (Figure 12b).

4. Conclusions

The growth process and luminescent and scintillation properties of CeAlO_3 single crystals have been considered in this work. We have shown the possibility of creating CeAlO_3 - $\text{CeAl}_{11}\text{O}_{18}$ -based scintillating metamaterials using the combination of the EFG growth method and post-growth high-temperature annealing of CeAlO_3 crystals in a reducing atmosphere or in vacuum.

Cathodoluminescence and radioluminescence in CeAlO_3 single crystals under e-beam excitation and α -particles excitation were registered for the first time. Under such types of excitation, CeAlO_3 single crystals possess double peaked luminescence in the visible range at 440 and 500 nm. This is related to Ce^{3+} 5d–4f transition in the $\text{CeAl}_{11}\text{O}_{18}$ phase, which is present in CeAlO_3 crystals as an admixture. The CL and RL intensity significantly increased in CeAlO_3 crystals after annealing at 1700 °C in an Ar and CO reducing atmosphere. Such annealed CeAlO_3 crystal also showed more intense thermoluminescence peaks in the 130–150 °C and 220–225 °C ranges, due to the larger concentration of oxygen vacancies and related traps compared to the as-grown counterpart.

We have also found that CeAlO_3 crystals show a quite fast scintillation response under α -particle excitation, with a decay time about of 56 ns. However, the scintillation light yield of annealed CeAlO_3 crystals is not high and equal to 310–315 photon/MeV under α -particle excitation by a ^{239}Pu (5.15 MeV) source. At the same time, after the optimization of growth and thermal treatment conditions, the heavy CeAlO_3 single crystal scintillators are promising for selective registration of high-energy particles, namely in the form of thin (up to 1 mm) plates, or could be used as the substrates in composite film-substrate scintillators based on the liquid phase epitaxy (LPE) grown structures of perovskite compounds [11,12].

Author Contributions: O.S. and Y.Z. analyzed experimental materials and wrote the test of the text the paper. P.A., S.T., I.G., and G.T. performed the experiments on growth of single crystals and metaphase materials, as well as co-wrote the growth part of the paper. T.Z. performed the luminescence and scintillation measurements. W.G. and P.B. performed the TSL measurements. P.M. performed SEM study and element analysis. A.P. performed XRD analysis.

Funding: The work was supported by the Polish NCN 2016/21/B/ST8/03200 and Ukrainian MES SL-76 F projects.

Conflicts of Interest: The authors declare no conflict of interest.

References

1. Irvine, J.T.S.; Connor, P. *Solid Oxide Fuels Cells: Facts and Figures, Green Energy and Technology*; Springer-Verlag: London, UK, 2013.
2. Arhipov, P.; Tkachenko, S.; Gerasymov, I.; Sidletskiy, O.; Hubenko, K.; Vasyukov, S.; Shiran, N.; Baumer, V.; Mateychenko, P.; Fedorchenko, A.; et al. Growth and characterization of large CeAlO₃ perovskite crystals. *J. Cryst. Growth* **2015**, *430*, 116–121. [[CrossRef](#)]
3. Pawlak, D.A. Metamaterials and photonic crystals—Potential applications for self-organized eutectic micro- and nanostructures. *Sci. Plena* **2018**, *4*, 014801.
4. Ohashi, Y.; Yasui, N.; Yokota, Y.; Yoshikawa, A.; Den, T. Submicron-diameter phase-separated scintillator fibers for high-resolution X-ray imaging. *Appl. Phys. Lett.* **2013**, *102*, 051907. [[CrossRef](#)]
5. Yasui, N.; Ohashi, Y.; Den, T.; Horie, R. Scintillator body, method for manufacturing the same, and radiation detector. Patent WO 2011/093176 A2, 4 August 2011.
6. Hishinuma, K.; Kamada, K.; Kurosawa, S.; Yamaji, A.; Pejchal, J.; Yokota, Y.; Ohashi, Y.; Yoshikawa, A. LiF/CaF₂/LiBaF₃ ternary fluoride eutectic scintillator. *Jpn. J. Appl. Phys.* **2015**, *54*, 04DH04. [[CrossRef](#)]
7. Cuneyt, T.A.; Akinc, M. Phase relations in the system Ce₂O₃-Al₂O₃ in inert and reducing atmospheres. *J. Am. Chem. Soc.* **1994**, *77*, 2961–2967.
8. Merker, L.; Herrington, K.D. Transmission spectra of rare earth titanates and aluminates. *Appl. Opt.* **1964**, *3*, 1311–1313. [[CrossRef](#)]
9. Blasse, G.; Grabmaier, B.C. *Luminescent Materials*; Springer: Berlin/Heidelberg, Germany, 1994.
10. Zorenko, Y.; Gorbenko, V.; Zorenko, T.; Voznyak, T.; Riva, F.; Douissard, P.A.; Martin, T.; Fedorov, A.; Suchocki, A.; Zhydachevski, Y. Growth and luminescent properties of single crystalline films of Ce³⁺ doped Pr_{1-x}Lu_xAlO₃ and Gd_{1-x}Lu_xAlO₃ perovskites. *J. Cryst. Growth* **2017**, *457*, 220–226. [[CrossRef](#)]
11. Witkiewicz-Lukaszek, S.; Gorbenko, V.; Zorenko, T.; Sidletskiy, O.; Gerasymov, I.; Fedorov, A.; Yoshikawa, A.; Mares, J.A.; Nikl, M.; Zorenko, Y. Development of composite scintillators based on single crystalline films and crystals of ce³⁺-doped (Lu,Gd)₃(Al,Ga)₅O₁₂ mixed garnet compounds. *Cryst. Growth Des.* **2018**, *18*, 1834–1842. [[CrossRef](#)]
12. Witkiewicz-Lukaszek, S.; Gorbenko, V.; Zorenko, T.; Paprocki, K.; Sidletskiy, O.; Gerasymov, I.; Mares, J.A.; Kucerkova, R.; Nikl, M.; Zorenko, Y. Novel all-solid-state composite scintillators based on the epitaxial structures of LuAG garnet doped with Pr, Sc, and Ce Ions. *IEEE Trans. Nucl. Sci.* **2018**, *65*, 2114–2119. [[CrossRef](#)]



© 2019 by the authors. Licensee MDPI, Basel, Switzerland. This article is an open access article distributed under the terms and conditions of the Creative Commons Attribution (CC BY) license (<http://creativecommons.org/licenses/by/4.0/>).